Supplementary Information

In Mie-theory simulation, the refractive index (RI) of BC core was set to be 1.56+0.47i according to Dalzell and Sarofim (1969) and the real part of RI was 1.52 for clear shell. Regarding to BrC, the RI is expected to show wavelength dependency and here the RI of brown shell was set to be $1.52+k_{brn}\cdot i$, where k_{brn} varies with wavelengths and it was deduced from Barnard et al. (2008) (Figure S1). Mie-theory simulations were conducted firstly for single particles. It is noticed in Figure 1 is that for Vp/Vc=1.0, which means pure BC core (also shown in Figure S2a), both $AAE_{370\text{-}520}$ and $AAE_{520\text{-}880}$ change non-monotonously with Dc. When BC core is small (<20 nm), $AAE_{370\text{-}520}$ and $AAE_{520\text{-}880}$ are close to 1.0, while they both increase as Dc gets larger and can be up to about 1.15. $AAE_{370\text{-}520}$ and $AAE_{520\text{-}880}$ reach to peak value at different Dc (around 75 nm and 115 nm, respectively) and then drop to lower than 1.0 for larger Dc.

To explain the varying AAE of pure BC particles, optical interpretation is performed based on Mie-theory as shown in Figure S3, where the wavelengths (λ_1 and λ_2) 370 nm and 520 nm are used as an example. Firstly, for a given two wavelengths λ_1 and λ_2, $AAE_{\lambda1\text{-}\lambda2}$ can be calculated from *Eq. 3,* where $b_{abs} = \mathrm{MAE} \cdot \frac{\pi\rho}{6} \cdot {D_c}^3$. Therefore, *Eq. 3* can be transferred into the following equation:

$$\mathrm{AAE}_{\lambda1-\lambda2} = -\frac{\ln(MAE_{\lambda1}\cdot\frac{\pi\rho}{6}\cdot {D_c}^3)-\ln(MAE_{\lambda2}\cdot\frac{\pi\rho}{6}\cdot {D_c}^3)}{\ln(\lambda1)-\ln(\lambda2)} = -\frac{\ln(MAE_{\lambda1})-\ln(MAE_{\lambda2})}{\ln(\lambda1)-\ln(\lambda2)} \qquad \textit{Eq. S1}$$

that is, $\mathrm{AAE}_{\lambda1-\lambda2} \propto \Delta\ \ln(MAE)_{\lambda1-\lambda2}$, as shown in Figure S3 where MAE is plotted in logarithmic axis. When Dc << λ, the entire particle mass participates in absorption and MAE is a constant, while for Dc >> λ, only the particle's skin contributes to absorption and MAE is inversely proportional to Dc (Bond and Bergstrom, 2006;Moosmuller and Arnott, 2009), therefore, the overall changing pattern of MAE is firstly keeping steady and then drop as a function of Dc. The slight peak of MAE before dropping is due to internal resonances (Moosmüller et al., 2009). Hence, whether AAE increases or decreases with Dc can be determined by comparing the first derivative of MAE at λ_1 and λ_2 (shown in the lower axis in Figure S3), which represents the slope of MAE for each Dc. The crossing point of slope_MAE is therefore corresponding to the maximum $AAE_{\lambda1-\lambda2}$, with core size of Dc_{max}. For example, when λ_1 and λ_2 are 370 nm and 520 nm, the maximum $AAE_{370-520}$ occurs when $Dc_{max} = Dc_0 = 75$ nm. AAE increases with Dc when $Dc < Dc_0$ but decreases when $Dc > Dc_0$. Since the slope_MAE at different wavelengths are in the same shape only shifting horizontally with longer wavelength, for AAE between longer wavelengths, Dc_{max} is larger (e.g. for AAE between 520 nm-880 nm, $Dc_{max} = Dc_1 = 115$ nm, Figure S3).

Above results clearly suggest that AAE of both pure BC particles or clear coated BC can be affected by their sizes and it is not a monotonous change and therefore assuming AAE as a constant is not adaptable. Time series of computed b_{abs_BrC} assuming $AAE_{BC} = 1.0$ can be found in Figure S5 and compared with the results using modified method.

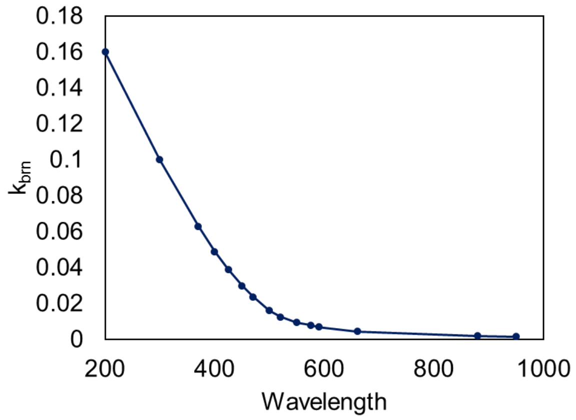

Figure S1. k_{brn} of brown shell (Barnard et al., 2008)

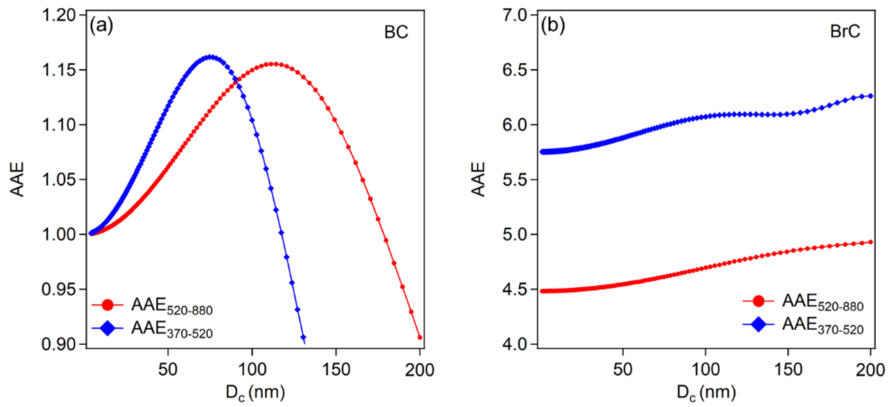

Figure S2. Absorption Angstroem Exponents between 370 and 520 nm ($AAE_{370\text{-}520}$) and between 520 and 880 nm ($AAE_{520\text{-}880}$) versus particle diameter (Dc), simulated by Mie model for pure (a) black carbon (BC) and (b) brown carbon (BrC) particles.

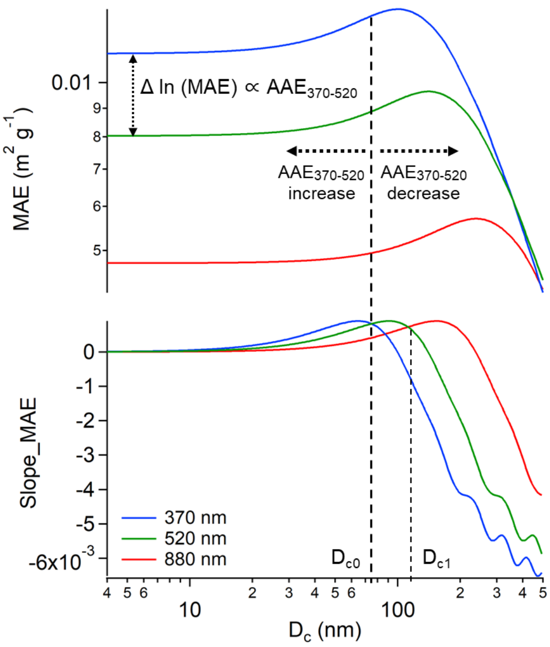

Figure S3. Variation of mass absorption efficiency (MAE) and slope of MAE (slope_MAE) vs. particle diameter (Dc) at 370 nm (λ_1), 520 nm (λ_2) and 880 nm for single pure black carbon (BC) at different Dc.

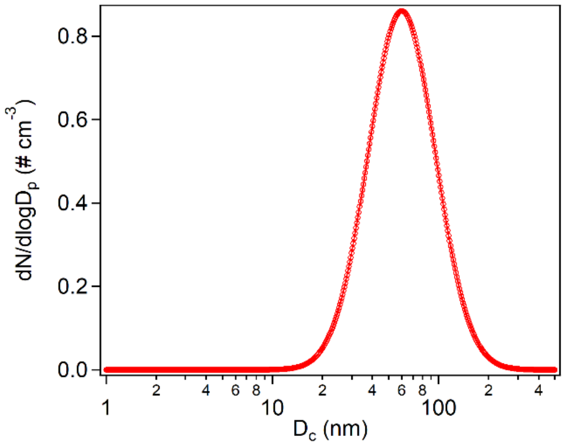

Figure S4. Lognormal number size distribution of BC cores assumed in Mie simulation

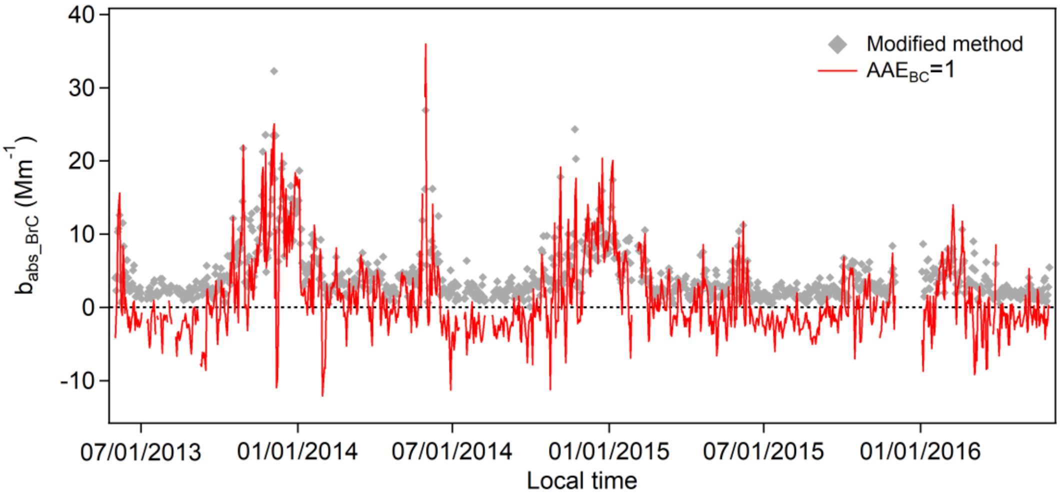

Figure S5. Time series of calculated b_{abs_BrC} assuming AAE_{BC}=1) versus using modified method

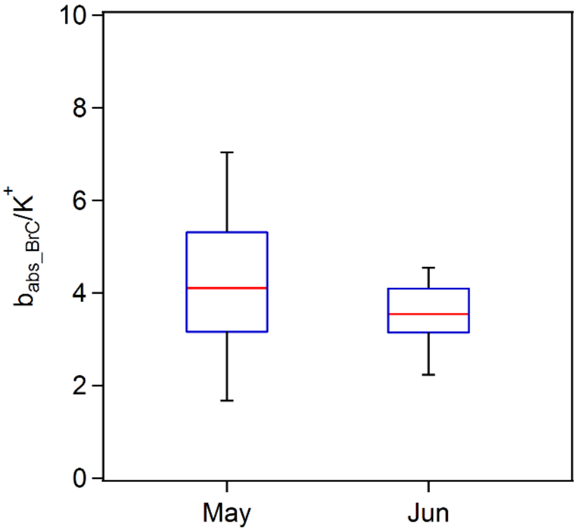

Figure S6. Significant difference result of b_{abs_BrC}/K^{+} in May and June (data is all from the year 2014)

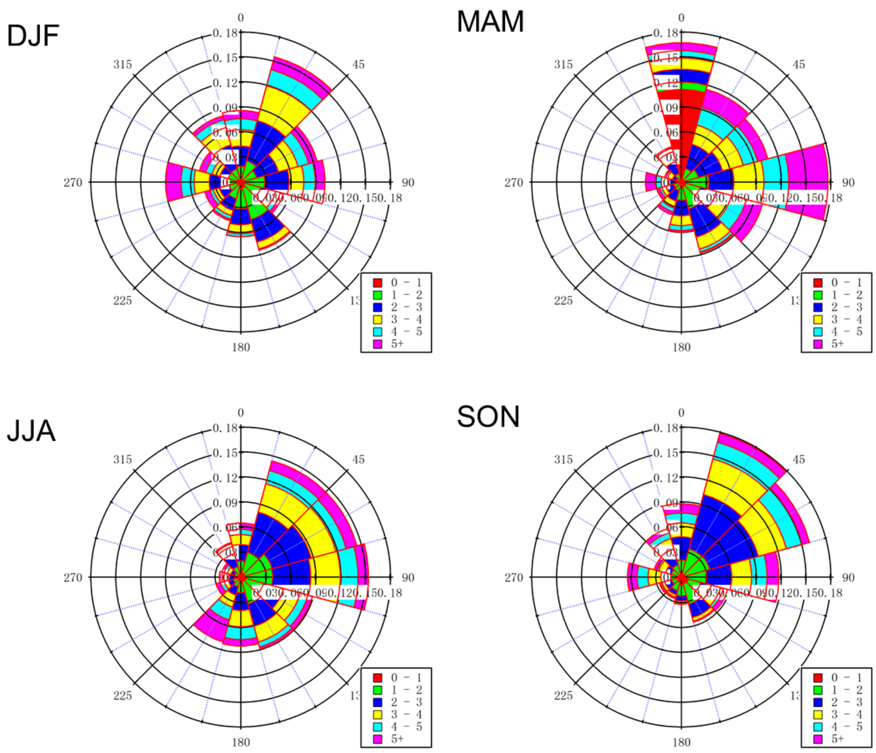

Figure S7. Wind roses at the SORPES station in four seasons

Table S1. Measured and simulated MAE at 370 nm, 520 nm, and 880 nm (in $m^2 g^{-1}$)

		370 nm	520 nm	880 nm
Measured (DJF)		11.4	7.2	4.2
Measured (JJA)		8.6	6.0	3.8
Simulated (brown shell)	D_p/D_c=1.5	10.4	6.3	3.2
	D_p/D_c =2.0	17.2	8.3	3.8
Simulated (clear shell)	D_p/D_c =1.5	8.6	6.0	3.1
	D_p/D_c =2.0	10.2	6.2	3.7

References

Barnard, J. C., Volkamer, R., and Kassianov, E. I.: Estimation of the mass absorption cross section of the organic carbon component of aerosols in the Mexico City Metropolitan Area, Atmos. Chem. Phys., 8, 6665-6679, https://doi.org/10.5194/acp-8-6665-2008, 2008.

Bond, T. C., and Bergstrom, R. W.: Light Absorption by Carbonaceous Particles: An Investigative Review, Aerosol Sci. Technol., 40, 27-67, 10.1080/02786820500421521, 2006.

Moosmüller, H., Chakrabarty, R. K., and Arnott, W. P.: Aerosol light absorption and its measurement: A review, J. Quant. Spectrosc. Radiat. Transfer, 110, 844-878, https://doi.org/10.1016/j.jqsrt.2009.02.035, 2009.

Moosmuller, H., and Arnott, W. P.: Particle optics in the Rayleigh regime, J. Air Waste manage., 59, 1028-1031, 10.3155/1047-3289.59.9.1028, 2009.